



ZIBELINE INTERNATIONAL

ISSN: 2521-0920 (Print)

ISSN: 2521-0602 (Online)

CODEN: MJGAAN



RESEARCH ARTICLE

PERMEABILITY-POROSITY TRENDS IN CAWC RESERVOIR SANDS IN THE NIGER DELTA NIGERIA, USING WELL-LOG DATA

Chinedu S. Orji, Etim D. Uko, Iyeneomie Tamunobereton-ari

Department of Physics, Rivers State University, PMB 5080, Port Harcourt, Rivers State, Nigeria.

*Corresponding Author Email: cstephenorji@gmail.com, e_uko@yahoo.com, tamunoberetonari@yahoo.com

This is an open access article distributed under the Creative Commons Attribution License, which permits unrestricted use, distribution, and reproduction in any medium, provided the original work is properly cited.

ARTICLE DETAILS

ABSTRACT

Article History:

Received 01 April 2019

Accepted 03 May 2019

Available online 09 May 2019

Reservoir characteristics analysis in the onshore Cawthorne Channel (CAWC) oil field, Niger Delta is here presented. The aim of the research was to assess reservoir properties and their relationships. A suite of geophysical logs comprising gamma ray, resistivity, neutron and density logs from eight wells were used in the analysis. Three reservoir sands were delineated and linked across all eight wells. The litho-stratigraphy correlation section revealed that each of the sand units spreads over the field are differs in thickness with some units occurring at greater depth than their adjacent unit, that is possibly an evidence of faulting. The results show volume of shale values range from 11% to 17% indicating that the fraction of shale in the reservoirs is quite low. The total porosity of the reservoirs ranges from 0.22 to 0.39 indicating a very good reservoir quality and reflecting probably well sorted coarse-grained sandstone reservoirs. The permeability of the reservoirs ranges from 288 mD to 1250mD and this suggests good reservoir horizons. The hydrocarbon saturation of the reservoirs ranges from 0.59 to 0.71 indicating that the proportion of void spaces occupied by water is low consequently high hydrocarbon production. Sand-shale lithology was calculated, with sandstone volume decreasing with increasing depth, while shale volume increases with depth. Porosity and permeability showed decreasing trend with depth for both sandstone and shale units in all wells with few exceptions. This could be as a result of low compaction by overburden pressure from overlying rocks. Plot of lithology versus depth reveals that shale lithology increases with depth, while sandstone decreases. Lithology versus porosity plots show an inverse relationship between permeability and shale volume and direct relationship between permeability and volume of sand. Lithology versus permeability shows that permeability and shale volume have an inverse relationship whereas permeability and volume of sand have a direct relationship. Permeability decreases exponentially with decrease in porosity in rock matrix made up of intercalation of sandstone and shale. The modelled equation of permeability and porosity is given by $K = 0.053e^{32.934\Phi}$. This implies that in the absence of core and well-log data, permeability can be estimated using only porosity data. The results of this work can be used as an exploration tool for the identification of prospective areas and also for feasibility studies during an appraisal activity.

KEYWORDS

Porosity, Permeability, Reservoir, Lithology, Nigeria

1. INTRODUCTION

Formation evaluation is used to understand the geology of the wellbore at high resolution and also to estimate the producible hydrocarbon reservoir. Formation evaluation is still a challenge in many fields because of the complexity of the reservoir environment subsequent diagenesis effect. Once formation evaluation is performed on the reservoir, it is crucial to pay attention to the location of the possible reservoir zone in the drilled section, determination of fluid type (gas, oil, water) present in the pore space, saturation level, and the mobility of the fluids across the connected pore space of the rock. To better achieve such information, it is important to have a good understanding of porosity (total, primary, effective porosity), water saturation computation, pay thickness and selection of cut offs. The aim of this process is to economically establish the existence of producible reservoirs. In this study, various well logs which include gamma ray, neutron, spontaneous potential, resistivity and density logs were analyzed and interpreted in order to define lithologic units of prospective zones, differentiating between hydrocarbon bearing and non-hydrocarbon bearing zone(s), and to investigate the relationship

between the petrophysical properties.

2. LOCATION AND GEOLOGY OF THE STUDY AREA

The Cawthorne Channel oil field is an onshore field in the coastal swamp depositional belt of the Niger Delta. Figure 1 shows the Cawthorne Channel oil field [1]. Its coordinates are Latitude 4°26'56.5" north and Longitude 7°5'1.8" east. The study area covers an area of 1,035 square kilometres and includes the Alakiri, Cawthorne Channel, Krakama, and Buguma Creek fields and related facilities. Comprising part mangrove swamp, the concession covers 1,035 km². Geologically, the study area lies in the eastern part of the Cenozoic Niger Delta (a typical wave and tidally dominated delta) where the main reservoirs are the sandstones of the heterolithic Agbada Formation (Eocene to Recent) deposited within delta-front, delta-topset, and fluvial-deltaic environments. The seismic data across the concession defines three mega structural trends; Northern (Alakiri, Buguma Creek, Orubiri and Asaritoru), Central (Krakama, Cawthorne Channel and Awoba) and Southern (no discoveries but at least one very good prospect identified).

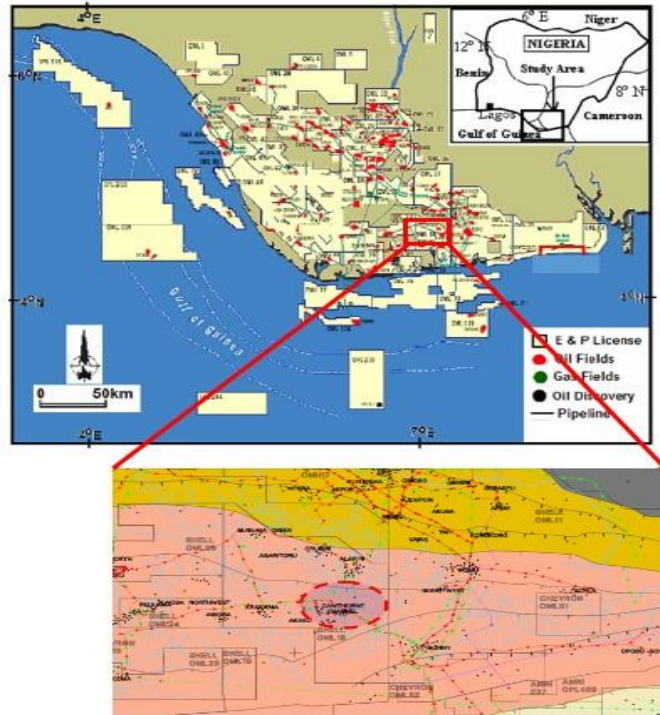


Figure 1: Map of the Niger Delta Showing Study Area [2]

3. MATERIALS AND METHODS

The data consist of well log suite which include calliper log, resistivity log, lithology logs (spontaneous log and gamma ray log), and porosity logs (sonic, neutron and density logs) from eight wells (CAWC 009, 013, 017, 021, 022, 023, 041 and 044). However, due to the gaps and null values in some wells, not all were used in the analysis. These data were analysed using Schlumberger Petrel. The methodology to estimate quantitative petrophysical properties from wireline log data using various rock physics models has the following stages: Well log preparation and editing, delineation of reservoir beds and well log correlation, petrophysical properties estimation and cluster analysis.

3.1 Delineation of Reservoir Beds

This is the process of determining reservoir zones with considerable hydrocarbon saturation. Logs respond to different lithologies. The gamma ray (GR) log is particularly useful for defining shale beds as well as the Spontaneous Potential (SP) log. The GR log reflects the proportion of shale and, in many regions, can be used quantitatively as a shale indicator.

3.2 Litho-stratigraphy correlation

A horizon represents an isochronous geologic time surface. It is the interface between two different rocks layers. It is associated with continuous and reliable reflection on the sections that appear over a large area. In order to perform a log analysis, it is necessary to pick the various zones of interest. In this study, selection of values was made on a consistent basis from day to day to assist reproducibility of results.

3.3 Computation of Petrophysical Properties

3.3.1 Volume of shale (Vsh)

Dresser proposed a new approach as a result of empirical correlation where the relationship changes according to the age or volume content of the formation. Younger rocks (Tertiary), unconsolidated [3]:

$$V_{sh} = 0.083 (2^{3.71GR} - 1) \tag{1}$$

V_{sh} = Volume of shale
 I_{GR} = Gamma-ray index

The gamma-ray index can be obtained from the linear equation:

$$I_{GR} = \frac{GR_{(log)} - GR_{(min)}}{GR_{(max)} - GR_{(min)}} \tag{2}$$

Where I_{GR} = Gamma-ray index; $GR_{(log)}$ = Gamma-ray reading from the log; $GR_{(min)}$ = Gamma-ray sand line; $GR_{(max)}$ = Gamma-ray shale line.

3.3.2 Total Porosity (Φ_T) and Effective Porosity (Φ_{eff})

In this work, the density log was used for the determination of the porosity by applying the equation [4]. Total Porosity was calculated from density porosity log using the equation:

$$\Phi_T = \frac{\rho_{ma} - \rho_b}{\rho_{ma} - \rho_f} \tag{3}$$

Where ρ_{ma} matrix density which is taken to be 2.65g/cc for sandstones [3]; ρ_b = Bulk density read directly from the log; ρ_f = the fluid density which is taken to be 1 for gas and 0.87 for oil. Effective Porosity is usually based

on an adjustment of total porosity by means of estimated shale volume (content) [3]:

$$\Phi_{eff} = \Phi_T - [\Phi_{sh} * V_{sh}] \tag{4}$$

where Φ_{eff} = effective porosity; Φ_T = total porosity; Φ_{sh} = log reading in a shale zone and V_{sh} = volume of shale.

3.3.3 Determination of Water Saturation (S_w)

Water Saturation is mathematically expressed as:

$$S_w = \left(\frac{a}{\Phi^m} \times \frac{R_w}{R_t} \right)^{\frac{1}{n}} \tag{5}$$

where S_w = Water saturation; a = Tortuosity factor; m = Cementation factor; n = Saturation exponent; Φ = Porosity of the formation; R_t = Deep resistivity of the formation.

3.3.4 Determination of Hydrocarbon Saturation (S_{hc})

The hydrocarbon saturation was deduced from water saturation by the following relationship:

$$S_{hc} = 1 - S_w \tag{6}$$

3.3.5 Determination of Permeability (K)

The permeability values for the observed reservoirs were calculated using the equation after method [5].

$$K^{1/2} = 250 \times \Phi^3 / S_{wirr} \tag{7}$$

where K = Permeability; Φ = Porosity; S_{wirr} = Irreducible water Saturation.

3.4 Cluster Analysis

Cross plot analysis was carried out to determine the rock properties/attributes that better discriminate the reservoir [6,7]. The goal of rock physics analysis is to determine the feasibility of discriminating between reservoir fluids and lithology of rock formations. Various cross plots were carried out. They include: depth versus lithology, depth versus porosity, depth versus permeability, lithology versus porosity, lithology versus permeability and porosity versus permeability.

4. RESULTS AND DISCUSSION

4.1 Reservoir Identification

The wells display a shale/sand/shale sequence which is characteristic of the Niger delta formation (Figures 2 to 10). The wells were analysed in terms of lithology from gamma ray log. Shale lithologies were defined by the high gamma ray value. Shale lithologies cause the deflection of resistivity to the far left due to its high conductive nature. It obvious that for every reservoir, porosity is generally high, signatures for volume of shale are low, water saturation are low while permeability are high as seen in the curves. This validates the expected log signatures of the properties of a productive reservoir.

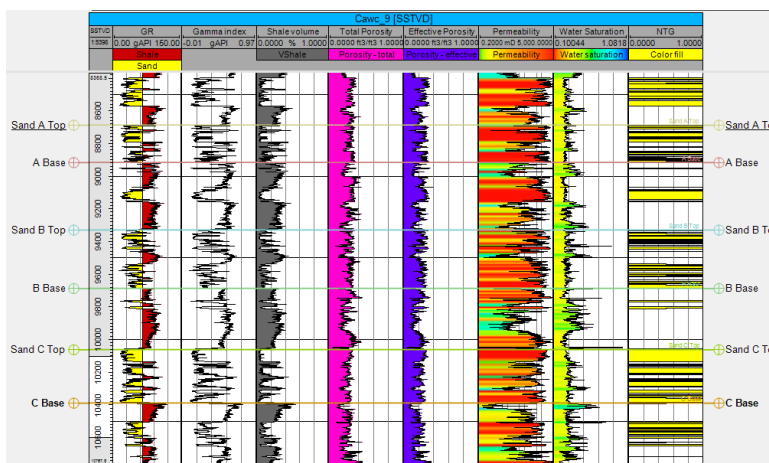


Figure 2: CAWC 9 Composite Well Logs

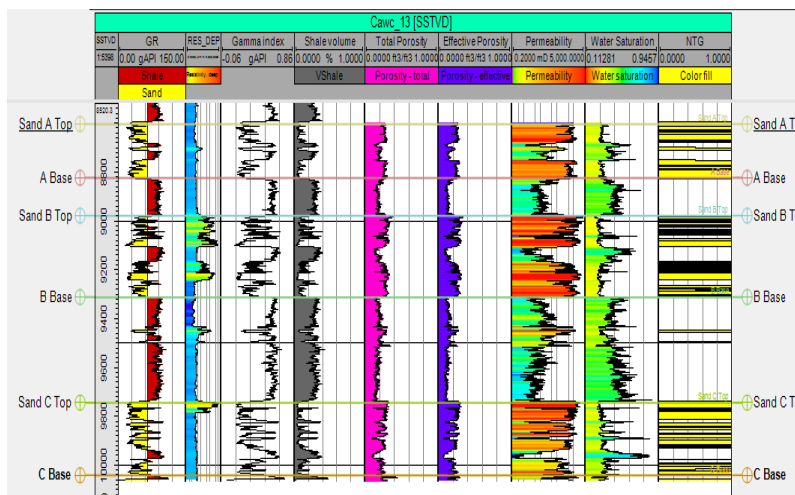


Figure 3: CAWC 13 Composite Well Logs

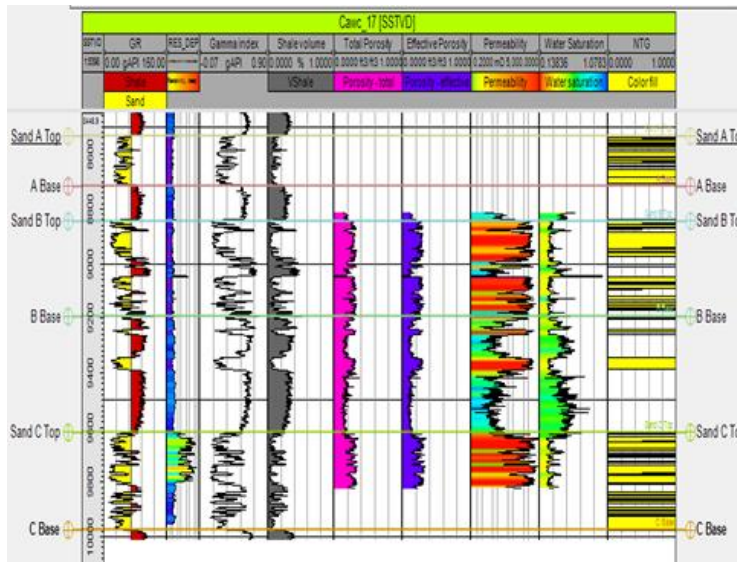


Figure 4: Cawc 17 Composite Well Logs

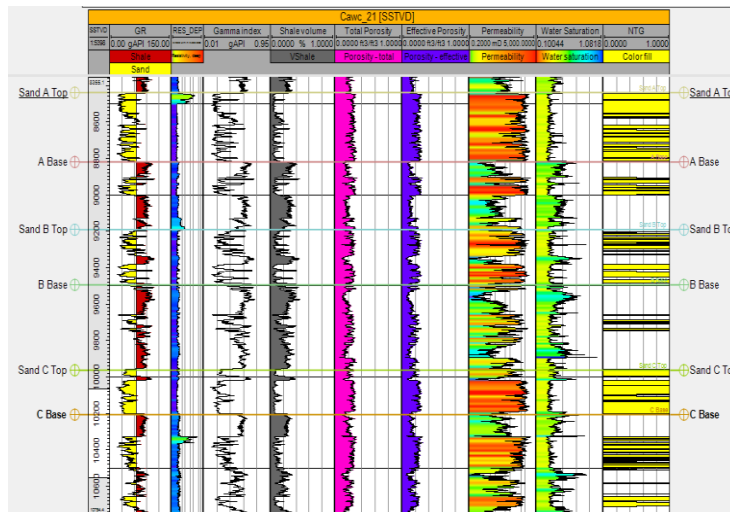


Figure 5: Cawc 21 Composite Well Logs

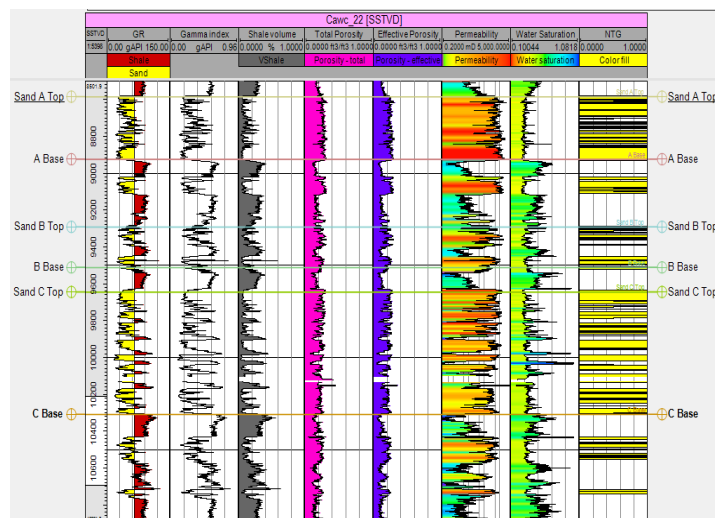


Figure 6: Cawc 22 Composite Well Logs

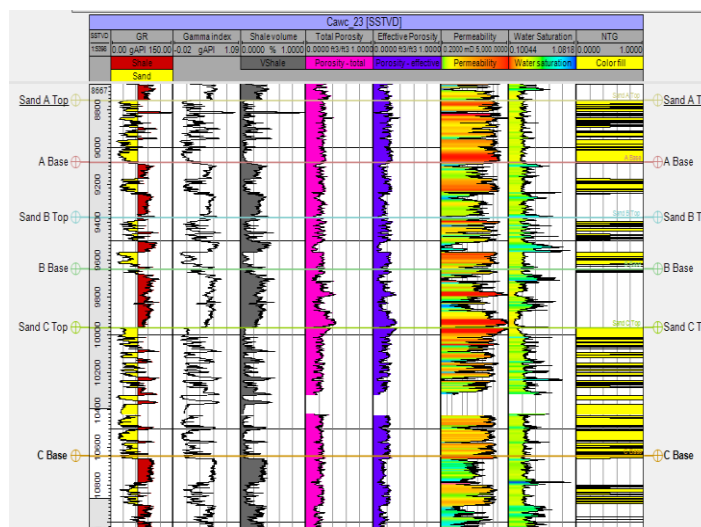


Figure 7: CAWC 23 Composite Well Logs

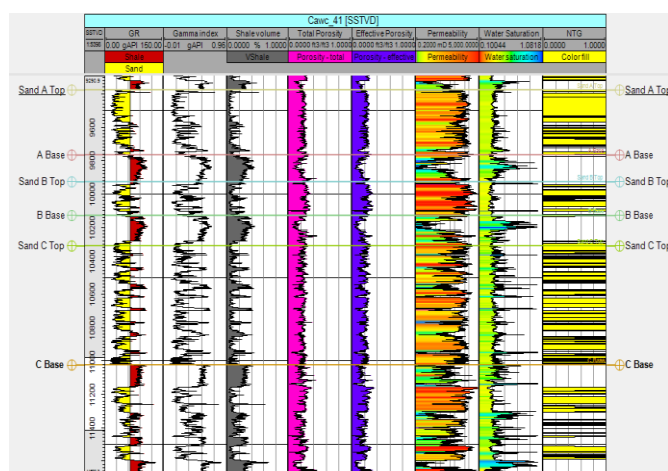


Figure 8: CAWC 41 Composite Well Log

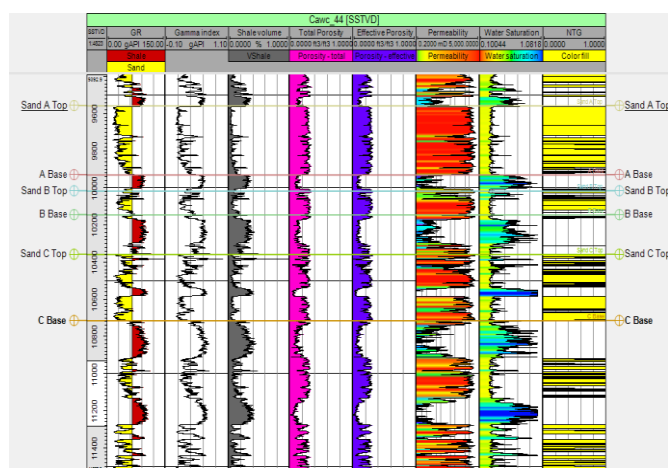


Figure 9: CAWC 44 Composite Well Logs

4.2 Lithologic Correlation

Lithologic units were identified on the logs and correlated across the wells. Lithology was interpreted based on gamma ray log signatures. Detailed observation of gamma ray logs shows progressive alternation of sand and shale. The stratigraphic cross-sections produced show a general lateral continuity of the lithologic units across the field. These surfaces were identified based on the abrupt change in well log properties – gamma-ray, resistivity and density among others. Three zones of interest (Sand A, Sand B and Sand C) were delineated and correlated across all eight wells. The litho-stratigraphy correlation section revealed that each of the sand units spreads over the field and differs in thickness with some units occurring at greater depth than their adjacent unit that is possibly

an evidence of faulting. The shale layers were observed to increase with depth along with a corresponding decrease in sand layers. This pattern in the Niger delta indicates a transition from Benin to Agbada Formation.

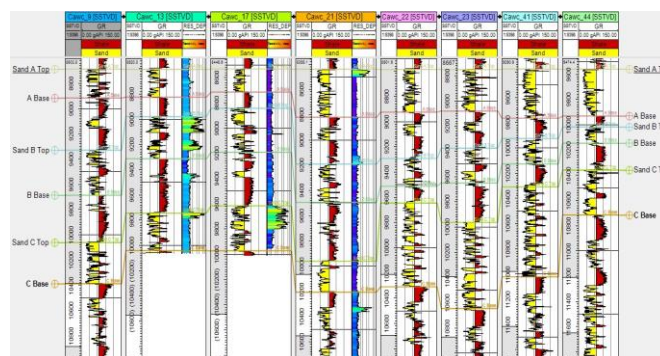


Figure 10: Lithologic Correlation Panel across Cawc Field for all Wells

4.3 Petrophysical Properties Evaluation

The computations were done using relevant equations and results obtained are presented in Tables 1 to 8. The wells are CACW 9, CACW 13, CACW 21, CACW 22, CACW 23, CACW 41 and CACW 44. After the wells were delineated, petrophysical properties were evaluated for each reservoir. The results obtained for the entire reservoirs are thus analysed.

The volume of shale was calculated from gamma ray index and the values range from 11% to 17% indicating that the fraction of shale in the reservoirs is quite low. The inference is the reservoir has a large volume of sand deposit than shale, therefore, hydrocarbon saturated. These reservoirs are good reservoir with high oil saturation at irreducible water saturation, because volume of shale values is low from 11% to 17%, which means that the sand body in all the reservoirs is high and there will be high rate of free flow of hydrocarbon in all the reservoirs as corroborated by their permeability values.

The total porosity of the reservoirs was estimated from density log (RHOB) using porosity formula and these values ranges from 0.22 to 0.39 indicating a very good reservoir quality and reflecting probably well sorted coarse-grained sandstone reservoirs with minimal cementation. The permeability of the reservoirs ranges from 288 md to 1250 Md. This implies that the permeability varies from very good to excellent and suggests that these are good (exploitable) reservoir horizon. For a rock to be considered as an exploitable hydrocarbon reservoir without stimulation, its permeability must be greater than approximately 100 md (however, depending on the nature of the hydrocarbon - gas reservoirs with lower permeabilities are still exploitable because of the lower viscosity of gas with respect to oil). This is as a result of very good to excellent sand quality.

The hydrocarbon saturation of the reservoirs ranges from 0.59 to 0.71 indicating that the proportion of void spaces occupied by water is low

consequently high hydrocarbon saturation and high hydrocarbon production. These results imply that the reservoir is highly porous and permeable. It also contains high hydrocarbons that is very viable for production. The curves of the various calculated petrophysical properties namely; NTG, Gamma Ray Index, Volume of Shale, Total/Effective Porosity, Water Saturation and Permeability for the wells studied are

presented in figures 4.18 to 4.26. It obvious that for every reservoir porosity are generally high, signatures for volume of shale are low, water saturation values are low while permeability values are high as seen in the curves. This validates the expected log signatures of the properties of a productive reservoir.

Table 1: Average petrophysical properties for CACW 9

| Reservoir Name | Top (ft) | Base (ft) | Volume of Shale (frac) | Φ_T (frac) | Φ_{eff} (frac) | S_w (frac) | S_h (frac) | K (mD) |
|----------------|----------|-----------|------------------------|-----------------|---------------------|--------------|--------------|---------|
| Sand A | 8680 | 8920 | 0.1607 | 0.2921 | 0.2485 | 0.2876 | 0.7124 | 1164.88 |
| Sand B | 9324 | 9680 | 0.1644 | 0.2838 | 0.2401 | 0.3018 | 0.6982 | 970.72 |
| Sand C | 10060 | 10390 | 0.1183 | 0.2668 | 0.2374 | 0.3151 | 0.6849 | 799.65 |

Table 2: Average petrophysical properties for CACW 13

| Reservoir Name | Top (ft) | Base (ft) | Volume of Shale (frac) | Φ_T (frac) | Φ_{eff} (frac) | S_w (frac) | S_h (frac) | K (mD) |
|----------------|----------|-----------|------------------------|-----------------|---------------------|--------------|--------------|--------|
| Sand 1 | 8600 | 8820 | 0.1244 | 0.2446 | 0.2174 | 0.3494 | 0.6506 | 535.55 |
| Sand 2 | 8980 | 9316 | 0.1598 | 0.2640 | 0.2267 | 0.3311 | 0.6689 | 840.08 |
| Sand 3 | 9740 | 10040 | 0.1293 | 0.2365 | 0.2101 | 0.3748 | 0.6252 | 528.59 |

Table 3: Average petrophysical properties for CACW 17

| Reservoir Name | Top (ft) | Base (ft) | Volume of Shale (frac) | Φ_T (frac) | Φ_{eff} (frac) | S_w (frac) | S_h (frac) | K (mD) |
|----------------|----------|-----------|------------------------|-----------------|---------------------|--------------|--------------|--------|
| Sand 1 | 8530 | 8715 | 0.1002 | GAPS | GAPS | GAPS | GAPS | GAPS |
| Sand 2 | 8840 | 9190 | 0.1552 | 0.2670 | 0.2294 | 0.3226 | 0.6774 | 793.90 |
| Sand 3 | 9610 | 9970 | 0.1115 | - | - | - | - | - |

Table 4: Average petrophysical properties for CACW 21

| Reservoir Name | Top (ft) MD | Base (ft) MD | Volume of Shale (frac) | Φ_T (frac) | Φ_{eff} (frac) | S_w (frac) | S_h (frac) | K (mD) |
|----------------|-------------|--------------|------------------------|-----------------|---------------------|--------------|--------------|--------|
| Sand 1 | | | | | | | | |
| Sand 2 | | | | | | | | |
| Sand 3 | | | | | | | | |

| | | | | | | | | |
|---------------|------|-------|--------|--------|--------|--------|--------|--------|
| Sand 1 | 8640 | 8820 | 0.0884 | 0.2652 | 0.2427 | 0.3167 | 0.6833 | 761.07 |
| Sand 2 | 9195 | 9500 | 0.1562 | 0.2392 | 0.2056 | 0.3635 | 0.6365 | 449.02 |
| Sand 3 | 9960 | 10210 | 0.1031 | 0.2483 | 0.2251 | 0.3442 | 0.6558 | 595.14 |

Table 5: Average petrophysical properties for CACW 22

| Reservoir Name | Top (ft) | Base (ft) | Volume of Shale (frac) | Φ_T (frac) | Φ_{eff} (frac) | S_w (frac) | S_h (frac) | K (mD) |
|----------------|----------|-----------|------------------------|-----------------|---------------------|--------------|--------------|---------|
| Sand 1 | 9590 | 9825 | 0.10556 | 0.27026 | 0.24239 | 0.3069 | 0.6931 | 707.294 |
| Sand 2 | 9290 | 9510 | 0.17036 | 0.22577 | 0.19124 | 0.38617 | 0.61383 | 348.464 |
| Sand 3 | 9650 | 10310 | - | - | - | - | - | 223.004 |

Table 6: Average petrophysical properties for CACW 23

| Reservoir Name | Top (ft) MD | Base (ft) MD | Volume of Shale (frac) | Φ_T (frac) | Φ_{eff} (frac) | S_w (frac) | S_h (frac) | K (mD) |
|----------------|-------------|--------------|------------------------|-----------------|---------------------|--------------|--------------|---------|
| Sand 1 | 8750 | 9080 | 0.12511 | 0.26217 | 0.23054 | 0.3185 | 0.681498 | 649.339 |
| Sand 2 | 9380 | 9650 | 0.17876 | 0.21918 | 0.18515 | 0.41001 | 0.589986 | 319.946 |
| Sand 3 | 9960 | 10650 | - | - | - | - | - | 288.968 |

Table 7: Average petrophysical properties for CACW 41

| Reservoir Name | Top (ft) | Base (ft) | Volume of Shale (frac) | Φ_T (frac) | Φ_{eff} (frac) | S_w (frac) | S_h (frac) | K (mD) |
|----------------|----------|-----------|------------------------|-----------------|---------------------|--------------|--------------|----------|
| Sand 1 | 9380 | 9760 | 0.09077 | 0.24214 | 0.22145 | 0.34566 | 0.654343 | 449.6013 |
| Sand 2 | 9923 | 10120 | 0.1262 | 0.27863 | 0.24511 | - | - | 998.1756 |
| Sand 3 | 10310 | 11020 | 0.12449 | 0.2291 | 0.20333 | 0.37552 | 0.624484 | 353.97 |

Table 8: Average petrophysical properties for CACW 44

| Reservoir Name | Top (ft) | Base (ft) | Volume of Shale (frac) | Φ_T (frac) | Φ_{eff} (frac) | S_w (frac) | S_h (frac) | K (mD) |
|----------------|----------|-----------|------------------------|-----------------|---------------------|--------------|--------------|----------|
| Sand 1 | 9380 | 9760 | 0.09077 | 0.24214 | 0.22145 | 0.34566 | 0.654343 | 449.6013 |
| Sand 2 | 9923 | 10120 | 0.1262 | 0.27863 | 0.24511 | - | - | 998.1756 |
| Sand 3 | 10310 | 11020 | 0.12449 | 0.2291 | 0.20333 | 0.37552 | 0.624484 | 353.97 |

| | Shale | | (frac) | | | | | |
|---------------|-------|-------|--------|--------|--------|--------|--------|---------|
| Sand 1 | 9560 | 9930 | 0.0773 | 0.2872 | 0.2661 | 0.2920 | 0.7080 | 1250.37 |
| Sand 2 | 10020 | 10140 | 0.1132 | 0.2822 | 0.2530 | 0.3135 | 0.6865 | 1205.63 |
| Sand 3 | 10360 | 10720 | 0.1284 | 0.2403 | 0.2156 | 0.4022 | 0.5978 | 754.01 |

4.4 Cluster Analysis

4.4.1 Delineation of Reservoirs

The top and base of the identified reservoirs of interest for Wells CACW 9, CACW 13, CACW 21, CACW 22, CACW 23, CACW 41 and CACW 44 are shown in Table 1-8. Three reservoirs each were delineated for each well, which adds up to twenty-four reservoirs. The wells display a shale/sand/shale sequence which is characteristic of the Niger delta formation. The wells were analyzed in terms of lithology from gamma ray log. Shale lithologies were defined by the high gamma ray value. Shale lithologies cause the deflection of resistivity to the far left due to its high conductive nature. Regions showing low gamma ray, high resistivity are mapped as sand lithologies.

4.4.2 Porosity-Depth Relations

Porosities decreases as the depth increases in all the reservoirs except for a few exceptions (Figure 11 show all wells). This could be as a result of low compaction by overburden pressure from overlying rocks or more non- interconnected pores spaces in the well. In the Niger Delta, shale lithology increases with depth, while sandstone decreases. Our observation confirms the results of porosity is lost with increasing depth of burial [8-10].

4.4.3 Permeability-Depth Relations

Figure 12 shows permeability-depth cross-plots. There is a normal linear decrease of permeability with an increase in depth, but within the Sand A and C of CAWC 9, there is an increase of permeability with an increase in depth as shown in the trend line of the depth-permeability cross-plot. This indicates an excellent permeability which is a property of highly prolific reservoirs.

4.4.4 Depth- Lithology Relations

The percentages of sandstones and shales (inferred to be lithology) were estimated using gamma ray logs. The graph of depth against volume of shale and sand were plotted and is shown in Figure 13. Clean sands (sand stones) are delineated as log signatures increasing towards the sand-line that is low. Hence, from the plots we can that the reservoirs are composed of sand stones with small pockets of shale. These plots show normal porosity decrease with depth. In the Niger Delta, shale lithology increases with depth, while sandstone decreases. Our observation confirms the results of shale lithology increases with increasing depth of burial [8-10].

3.4.5 Lithology-Porosity Relations

Figure 14 is Lithology versus Total Porosity cross-plots for all wells. There is generally an inverse relationship between permeability and shale volume and direct relationship between permeability and volume of sand. Comparing both lithologies (Shale bed and sandstone bed) to the trend relationship, it was observed that approximately at same depth; shale is denser than sandstone; because shale undergoes plastic compaction or deformation while sandstone undergoes elastic compaction or deformation [11]. Also, our results show that shale porosity decreases with increase in depth [12-16].

4.4.6 Lithology-Permeability Relations

Figure 15 is the plot of permeability versus lithology for all wells. It is observed that permeability and shale volume have an inverse relationship whereas permeability and volume of sand have a direct relationship. The rate of shale compaction decreases with increase in burial [12-16]. This may be caused by decreasing shale permeability and increasing water viscosity, thus increasing rate of fluid expulsion with increasing compaction.

4.4.7 Porosity-Permeability Relations

Permeability decreases exponentially with decrease in porosity in rock matrix made up of intercalation of sandstone and shale as demonstrated in Figure 16. The modelled Equation of permeability and porosity is given by: $K = 0.053e32.934\Phi$. This implies that in the absence of core and well-log data, permeability can be estimated using only porosity information.

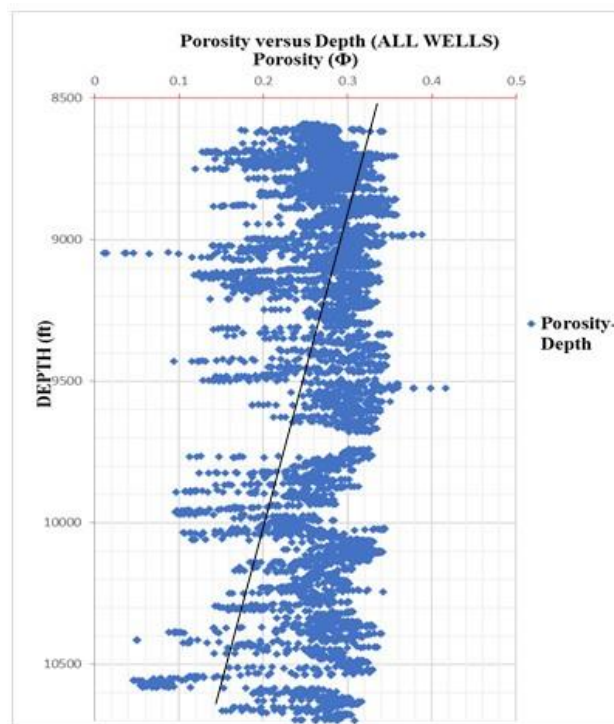


Figure 11: A Plot of Total Porosity versus Depth for all wells

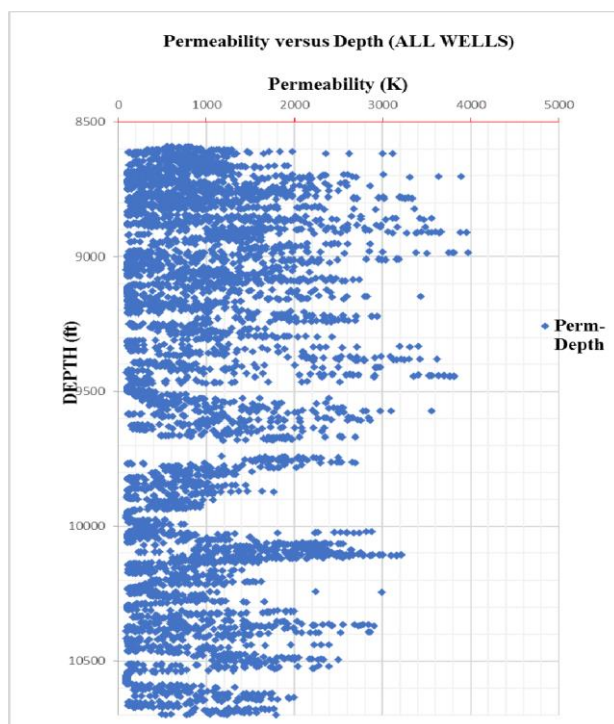


Figure 12: A Plot of Permeability versus Depth for all wells

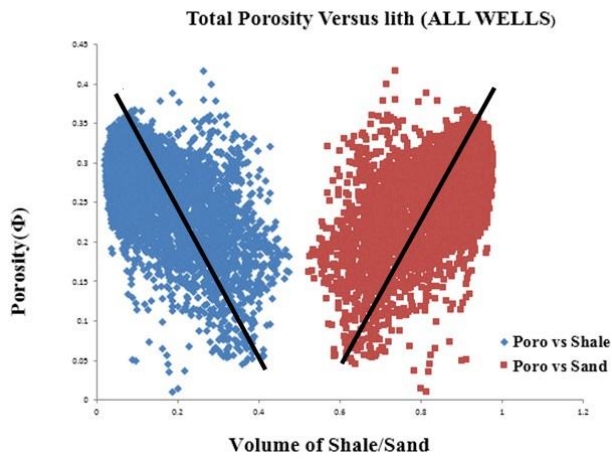


Figure 13: Total Porosity Versus lithology for all wells

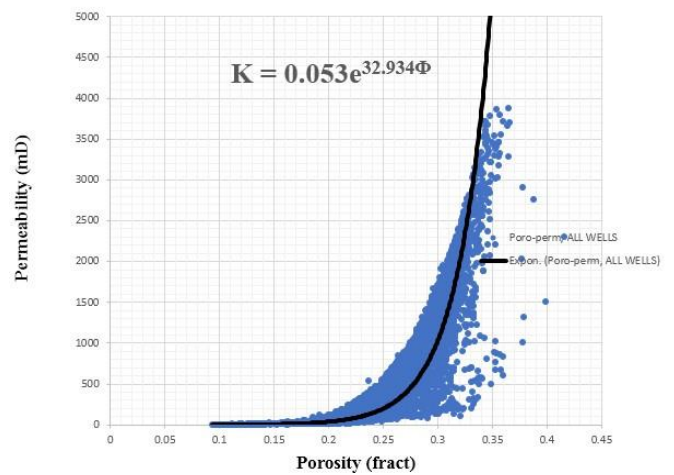


Figure 16: Permeability versus Porosity for all wells

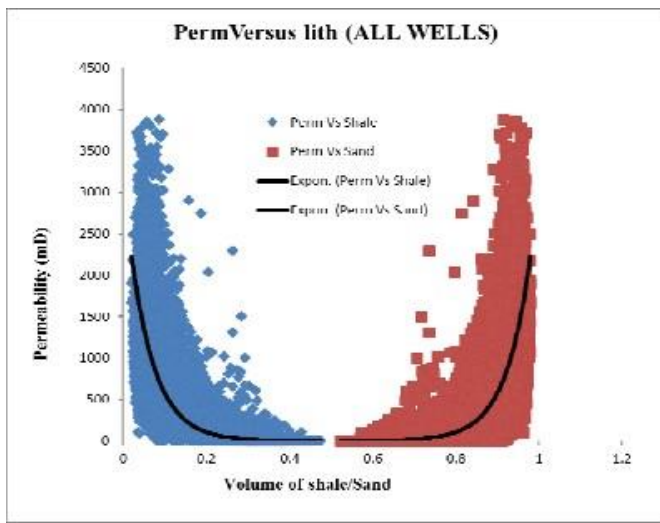


Figure 14: Permeability versus Lithology for all wells

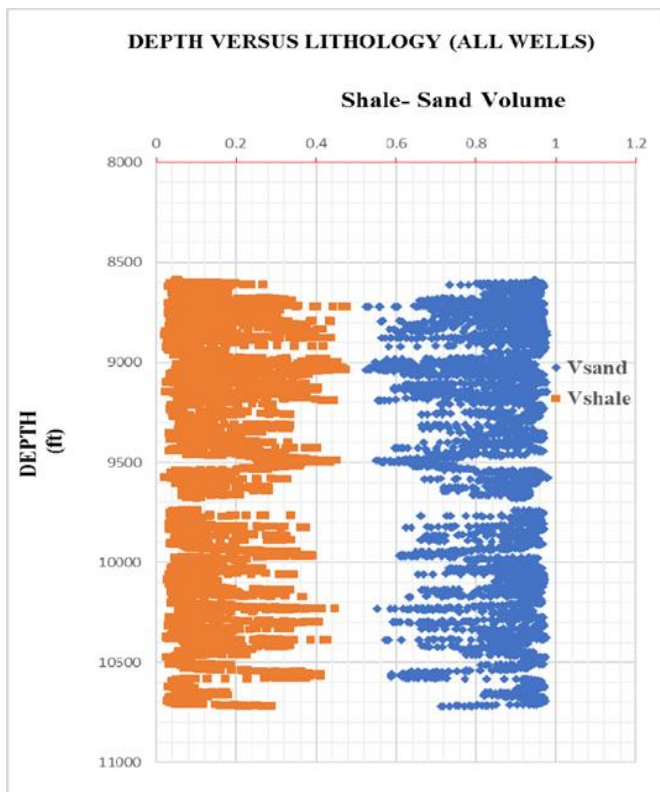


Figure 15: Depth-Lithology for all wells

5. CONCLUSION

Reservoir property study and assessment have been successfully done using well log data in Cawthorne Channel oil field, Onshore, Niger Delta to assess reservoir properties and their connection. Three zones of interest (Sand A, Sand B and Sand C) were delineated and correlated across all eight wells. The litho-stratigraphy correlation section revealed that each of the sand units spreads over the field and differs in thickness with some units occurring at greater depth than their adjacent unit that is possibly an evidence of faulting. The petrophysical parameters calculated include total/effective porosity, water/hydrocarbon saturation, permeability, net-to-gross and volume of shale. Also, graphs were plotted to investigate the relationship between the petrophysical properties in the cross-plot space. The results obtained show volume of shale values range from 11% to 17% indicating that the fraction of shale in the reservoirs is quite low. The total porosity of the reservoirs ranges from 0.22 to 0.39 indicating a very good reservoir quality and reflecting probably well sorted coarse-grained sandstone reservoirs with minimal cementation.

The permeability of the reservoirs ranges from 288 mD to 1250 mD. This implies that the permeability varies from very good to excellent and suggests that these are good (exploitable) reservoir horizon. The hydrocarbon saturation of the reservoirs ranges from 0.59 to 0.71 indicating that the proportion of void spaces occupied by water is low consequently high hydrocarbon saturation and high hydrocarbon production. These results imply that the reservoir is highly porous and permeable. It also contains high hydrocarbons that is very viable for production. Sand-shale lithology was calculated, with sandstone volume decreasing with increasing depth, while shale volume increases with depth.

Porosity and permeability showed decreasing trend with depth for both sandstone and shale units in all wells with few exceptions. This could be as a result of low compaction by overburden pressure from overlying rocks or more non-interconnected pores spaces in the well. Plot of lithology versus depth reveals that shale lithology increases with depth, while sandstone decreases. Lithology versus porosity plots show an inverse relationship between permeability and shale volume and direct relationship between permeability and volume of sand. Lithology versus permeability shows that permeability and shale volume have an inverse relationship whereas permeability and volume of sand have a direct relationship. Permeability decreases exponentially with decrease in porosity in rock matrix made up of intercalation of sandstone and shale. The modelled Equation of permeability and porosity is given by: $K = 0.053e^{32.934\Phi}$. This implies that in the absence of core and well-log data, permeability can be estimated using only porosity information. The results of this work can be used as an exploration tool for the identification or evaluation of prospective areas, locations and also for feasibility studies during an appraisal activity. This study also has proven that the estimation of petrophysical data is a key factor for effective productivity of hydrocarbons.

ACKNOWLEDGEMENT

The authors are thankful to Nigeria National Petroleum Company (NNPC) for the permission given to us to obtain data from The Shell Petroleum Development Company (SPDC) Nigeria Limited.

REFERENCES

- [1] Short, K.C., Stauble, A.J. 1967. Outline of geology of Niger Delta. American Association of Petroleum Geologists Bulletin, 51, 761-779.
- [2] Nton, M.E., Esan, T.B. 2010. Sequence Stratigraphy of EMI Fields, Offshore Eastern Niger Delta, Nigeria. European Journal of Scientific Research, 44 (1), 115 – 132.
- [3] Dresser, A. 1982. Well logging and interpretation techniques, the course for home study. Dresser Industries Inc, Houston.
- [4] Schlumberger, 1989. Log Interpretation, Principles and Application: Schlumberger Wireline and Testing, Houston, Texas, pp. 21-89.
- [5] Wyllie, M.R.J., Rose, W.D. 1989. Some theoretical considerations related to the quantitative evaluation of the physical characteristics of reservoir rock from electric log data. Trans AIME 189, 105p.
- [6] Singh, N.P. 2019. Permeability prediction from wireline logging and core data: a case study from Assam- Arakan basin. Journal of Petroleum Exploration and Production Technology, 9 (1), 97-305.
- [7] Omudu, L.M., Ebeniro, J.O. 2007. Cross-Plot and Descriptive Statistics for Lithology and Fluid Discrimination: A Case Study from Onshore Niger Delta: Presented at the Annual Meeting of Nigerian Association of Petroleum Explorationists (NAPE), Abuja, Nigeria.
- [8] Friedman, J.H., Sanders, J.E. 1978. Principles of Sedimentology J. Wiley & sons, New York.
- [9] Blatt, H., Middleton, G., Murray, R. 1980. Origin of Sedimentary Rocks, 2nd edition, Printice Hall, Inc., New Jersey, pp 782.
- [10] Selly, R.C. 1980. Introduction to Sedimentology, 2nd edition (Academic Press, London), pp. 475.
- [11] Tamunosiki, D., Han Ming, G.U., Liping, W., Uko, E.D., Warmate, T. 2014. Petrophysical Characteristics of Coastal Swamp Depobelt Reservoir in the Niger Delta Using Well-Log Data. Journal of Applied Geology and Geophysics, 2 (2), 76-85.
- [12] Magara, K. 1980. Comparism of Porosity depth relationships of shale and sandstone. Journal of Petroleum Geology, 3 (2).
- [13] Onuoha, C., Uko, E.D., Tamunobereton-ari, I. 2018. Determination of Lithology and Pore-Fluid of A Reservoir in Parts of Niger Delta Using Well-Log Data. Journal of Applied Physics, 10 (2), 71- 82.
- [14] Uko, E.D., Alabraba, M.A., Idahosa, L., Tamunosiki, D. 2017. Porosity-Permeability Relationship in the North-West Niger Delta Basin, Nigeria. World Journal of Applied Science and Technology, 9 (2), 150 – 159.
- [15] Uko, E.D., Dieokuma, T., Gu, H., Ming, I., Tamunobereton-ari, I., Emudianughe, J.E. 2015. Porosity Modelling of the South-East Niger Delta Basin, Nigeria. International Journal of Geology, Earth and Environmental Sciences, 4 (1), 49-60.
- [16] Boaca, T., Malureanu, I. 2017. Determination of oil reservoir permeability and porosity from resistivity measurement using an analytical model. Journal of Petroleum Science and Engineering, 157, 884- 893

